Organic Electronics 12 (2011) 802–808

Contents lists available at ScienceDirect

Organic Electronics

journal homepage: www.elsevier.com/locate/orgel

Efficient blue organic light-emitting diode using anthracene-derived emitters based on polycyclic aromatic hydrocarbons

Jong-Kwan Bin, Jong-In Hong *

Department of Chemistry, College of Natural Sciences, Seoul National University, Seoul 151-747, Republic of Korea

ARTICLE INFO

Article history:
Received 16 September 2010
Received in revised form 21 December 2010
Accepted 13 February 2011
Available online 26 February 2011

Keywords:
Organic light-emitting diode
Blue emission
Anthracene
Polycyclic aromatic hydrocarbons

ABSTRACT

We have synthesized two light-emitting materials based on polycyclic aromatic hydrocarbons (PAHs) for use in blue organic light-emitting diodes (OLEDs). 9-(Phenanthryl)-10-(3-(9-phenylcarbazole-9-yl)anthracene (PPCA) acts as the host and 9,10-bis-biphenyl-4-yl-2,6-diphenylanthracene (BDA) acts as the dopant. PPCA contains an electron-transporting phenanthrene moiety and a hole-transporting 9-phenyl-9H-carbazole moiety in the anthracene core. BDA contains PAHs without amino substituents in the anthracene core. The optimized device structure, ITO/DNTPD (600 Å)/α-NPB (300 Å)/PPCA:BDA 5 wt.% (250 Å)/N1PP (300 Å)/LiF (5 Å)/Al (1000 Å), is characterized by blue electroluminescence (EL), with a current efficiency of 6.9 cd/A, power efficiency of 3.23 lm/W, and external quantum efficiency of 5.1% at 10 mA/cm^2 and CIE coordinates of (0.15, 0.18).

Introduction

In recent years, considerable attention has been paid to the development of organic emissive materials for full-color display applications. A number of red- and green-light-emitting candidates have already been identified for organic light-emitting diodes (OLEDs); OLEDs based on these compounds are characterized by high luminous efficiency, reasonable color purity, and long lifetime. However, the development of blue OLEDs with high electroluminescence (EL) efficiency remains a challenge because of the requirement of a large band-gap energy. It is well known that a host-dopant system can significantly improve the device performance in terms of both EL efficiency and operational lifetime [1]. In general, there are two different types of dopants that can be used to realize blue light emission: polycyclic aromatic hydrocarbons (PAHs) with amino substituents and those without amino substituents. To date, there have been a number of reports on blue dopants with amino substituents, such as mono- and distyrylarylenes [2–4] and pyrene derivatives [5]. However, the use of PAHs without amino substituents as blue dopants has not been studied in detail. The band-gap energy of PAHs is determined by the conjugation length of the molecules. The advantages of PAHs include a high fluorescence quantum yield and dense packing ability [6]. Furthermore, it is known that electronic devices manufactured using PAHs are relatively stable. PAHs also help to increase the half-life of undoped and doped OLEDs by 30–150 times [7]. There have been several reports on the use of PAHs without amino substituents as EL emitters [8–10]. For example, Tseng and Yang used 7,8,10-triphenylfluoranthene (TPF) as the blue host and dipyrenylfluorene (DPF) as the blue dopant and achieved an EL efficiency of 3.33 cd/A and an external quantum efficiency of 2.48% at Commission International de L'Eclairage (CIE) coordinates of (0.164, 0.188) [8].

Among the blue-emitting materials, anthracene derivatives have been intensively studied for use as the blue host material in OLEDs because of their excellent photoluminescence (PL) and EL properties [11–14]. Additionally, the fluorescent color of anthracene can be easily changed from blue to green by introducing symmetric or asymmetric moieties at the C-9 and C-10 positions [15]. However, tetraaryl-substituted anthracene derivatives acting as blue

* Corresponding author. Tel.: +82 2 880 6682.
E-mail address: jihong@snu.ac.kr (J.-I. Hong).

1566-1199/$ - see front matter © 2011 Elsevier B.V. All rights reserved.
doi:10.1016/j.orgel.2011.02.011

light-emitting materials are rare. For example, a blue light emitter with four substituents at the 2,6,9,10-positions of anthracene (2,6-bis(9,9-diethyl-9H-fluoren-2-yl)-9,10-diphenylanthracene) has been proven to exhibit an EL efficiency of 5.8 cd/A and an external quantum efficiency of 2.11% [16]. Chen et al. synthesized 9,10-diphenylanthracene (DPA)-derived copolymers emitting blue light. The OLEDs fabricated using these DPA-derived copolymers exhibited sky-blue EL (at CIE coordinates of (0.19, 0.30)) with a peak luminous efficiency of 1.26 cd/A. Still, the development of OLEDs using anthracene-derived moieties remains a challenge [17].

Herein, we report the use of an anthracene-based blue host, 9-(phenanthryl)-10-(3-(9-phenylcarbazole-9-yl)anthracene (PPCA), and a dopant 9,10-bis-biphenyl-4-yl-2,6-diphenylanthracene (BDA) which contains PAHs without amino substituents (Schemes 1 and 2). Specifically, PPCA was synthesized from 9-phenyl-9H-carbazole, which possesses good hole-transporting properties, and phenanthrene, which has good electron-transporting properties [18]. We believe that the introduction of carbazole and phenanthrene elements in the 9,10-anthracene core of PPCA is an effective method for avoiding molecular aggregation and enhancing the efficiency of transporting electrons and holes (carriers). We examined the light-emitting performance in devices fabricated using aluminum tris(8-hydroxyquinoline) (Alq_3) and 1,6-di(pyridin-3-yl)-3,8-di(naphthalene-1-yl)pyrene (N1PP) [19] as electron-transport materials. In particular, with the use of N1PP, which shows high carrier mobility, the EL efficiency of the blue OLED devices based on PAHs without amino substituents was significantly improved.

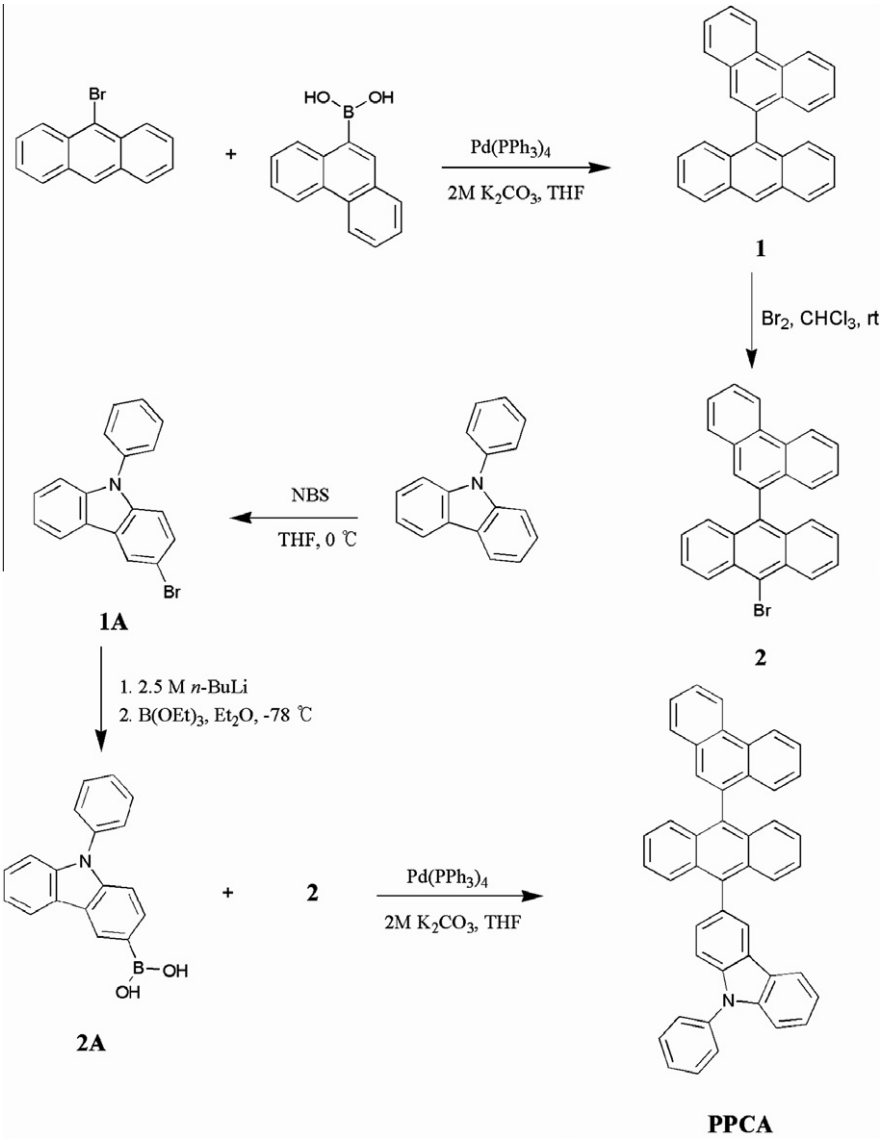

Scheme 1. Synthesis of PPCA.

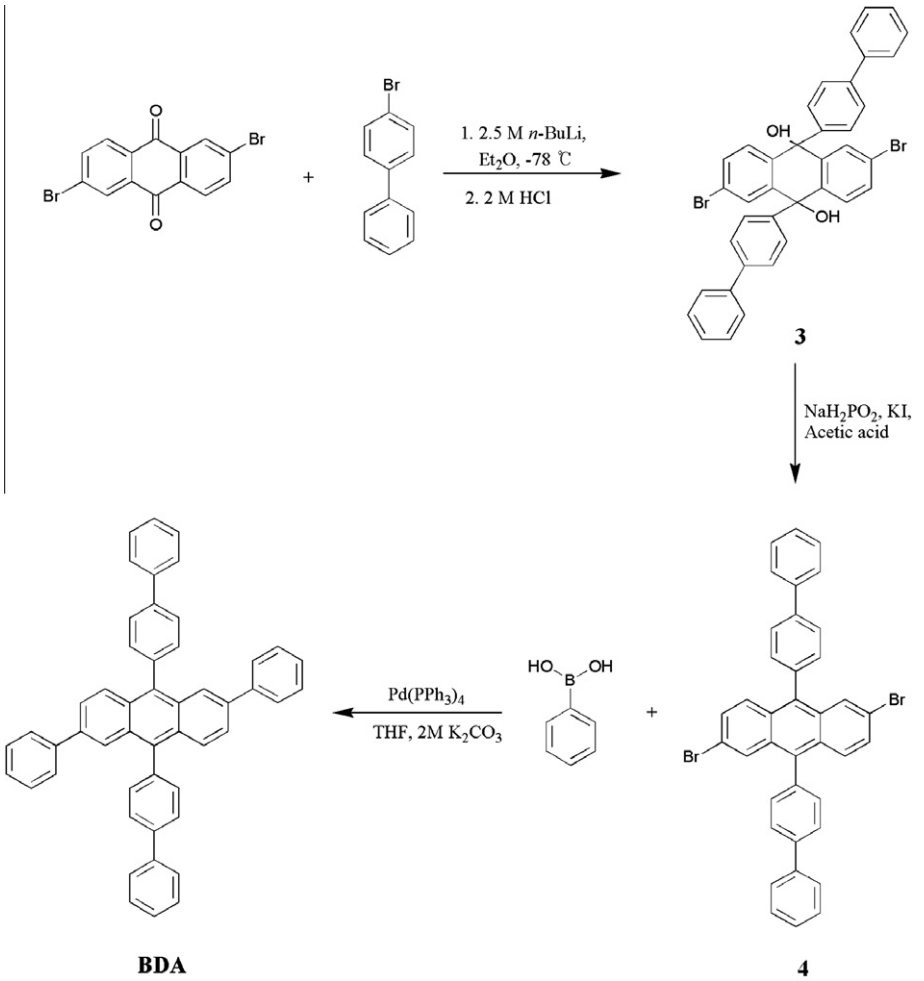

Scheme 2. Synthesis of BDA.

2. Experimental

2.1. Materials and instrument

9-Bromoanthracene, 9-phenanthreneboronic acid, 9-phenylcarbazole, and 4-bromobiphenyl were purchased from Tokyo Chemical Industry Co., Ltd., (TCI, Japan) and Aldrich Chemical Co., (USA). Compounds **1A**, **2A**, **3**, and **4** (Schemes 1 and 2) were synthesized according to literature methods as well as modified procedures [16,20]. Analytical thin-layer chromatography was performed using Kieselgel 60F-254 plates provided from Merck KGaA (Germany). Column chromatography was carried out on Merck silica gel 60 (70–230 mesh). All the solvents and reagents are commercially available and were used without further purification, unless otherwise noted. ^{1}H and ^{13}C nuclear magnetic resonance (NMR) spectra were recorded in $CDCl_3$ using a Bruker Advance 300 MHz spectrometer. Proton (^{1}H) NMR chemical shifts in $CDCl_3$ were referenced to $CHCl_3$ (7.27 ppm). Mass spectra were obtained by means of gas chromatography/high-resolution mass spectrometry. Ultraviolet and visible (UV–vis) absorption spectra were recorded with the use of a Beckman DU 650 spectrophotometer.

2.1.1. 9-Phenanthren-9-yl-anthracene (1)

A solution of 9-bromoanthracene (2 g, 7.78 mmol), 9-phenanthreneboronic acid (1.90 g, 8.56 mmol), $Pd(PPh_3)_4$ (3 mol%), and aqueous K_2CO_3 (10.8 g, 78 mmol, water 50 mL) in a toluene (10 mL)–tetrahydrofuran (THF, 50 mL) mixture was heated at a temperature of 100 °C for 10 h in a N_2 atmosphere. After the solvent was evaporated, the residue was treated with water and extracted with dichloromethane. The crude product was purified by silica gel column chromatography (10% dichloromethane (DCM) in *n*-hexane used as eluent) and further purified by recrystallization (yield: 87%). ^{1}H NMR (300 MHz, $CDCl_3$): δ (ppm) 7.18 (d, ^{1}H, J = 8.07 Hz), 7.24–7.35 (m, 3H), 7.49 (t, 2H, J = 7.4 Hz), 7.59 (d, 2H, J = 8.60 Hz), 7.75 (m, 2H), 7.80 (t, ^{1}H, J = 7.14 Hz), 7.86 (s, ^{1}H), 7.94 (d, ^{1}H, J = 7.73 Hz), 8.14 (d, 2H, 8.49 Hz), 8.78 (s, ^{1}H), 8.90 (d, 2H, J = 8.28 Hz).

2.1.2. 9-Bromo-10-phenanthren-9-yl-anthracene (2)

A solution of bromine (0.91 g, 5.70 mmol) in chloroform (20 mL) was slowly added to a solution of **1** (2 g, 5.64 mmol) in chloroform (50 mL) at room temperature. After stirring for 5 h, the mixture was poured into EtOH. The residue obtained after filtration was purified by flash chromatography using dichloromethane (yield: 89%). ^{1}H NMR (300 MHz, $CDCl_3$): δ (ppm) 7.13 (d, ^{1}H, J = 8.10 Hz), 7.26–7.34 (m, 3H), 7.56–7.73 (m, 6H), 7.68–7.81 (m, ^{1}H), 7.83 (s, ^{1}H), 7.93 (d, ^{1}H, J = 6.38 Hz), 8.70 (d, 2H, J = 8.82 Hz), 8.89 (d, 2H, J = 8.22 Hz).

2.1.3. 9-(Phenanthryl)-10-(3-(9-phenylcarbazole-9-yl)-anthracene (PPCA)

2A was allowed to react with **2** under Suzuki reaction conditions, as described in the synthesis of **1,** to afford PPCA (yield: 82%). ^{1}H NMR (300 MHz, $CDCl_3$): δ (ppm) 7.31–7.36 (m, 5H), 7.49–7.77 (m, 16H), 7.88–7.97 (m, 4H), 8.14–8.18 (m, ^{1}H), 8.39–8.32 (m, ^{1}H), 8.91 (d, 2H, J = 8.2 Hz); ^{13}C NMR (75 MHz, $CDCl_3$) δ 109.74, 109.77, 100.06, 120.21, 120.51, 122.78, 122.90, 123.19, 123.30, 12.55, 125.08, 125.30, 126.29, 126.74, 126.93, 127.0, 129.09, 127.23, 127.54, 127.65, 128.83, 129.37, 130.04, 130.45, 130.53, 130.69, 130.80, 131.82, 132.84, 134.65, 135.58, 137.78, 138.41, 140.41, 141.40; HRMS (FT MS) m/z: calcd. for $[C_{46}H_{29}N + H]^+$ 596.23, found $[M + H]^+$ 596.24; Anal. calcd. for $C_{46}H_{29}N$: C, 92.74; H, 4.91; N, 2.35. Found: C, 92.7033; H, 4.9502; N, 2.3309.

2.1.4. 9,10-Bis-biphenyl-4-yl-2,6-diphenylanthracene (BDA)

4 (2 g, 3.12 mmol) was allowed to react with phenylboronic acid (0.84 g, 6.87 mmol) under Suzuki reaction conditions, as described in the synthesis of PPCA, to afford BDA (yield: 72%); ^{1}H NMR (300 MHz, $CDCl_3$): δ (ppm) 7.33–7.42 (m, 8H), 7.53–7.73 (m, 14H), 7.81–7.91 (m, 10H), 8.01 (s, 2H); HRMS (FT MS) m/z: calcd. for $[C_{46}H_{29}N + H]^+$ 635.27, found $[M + H]^+$ 635.28. Anal. calcd. for $C_{50}H_{34}$: C, 94.60; H, 5.40. Found: C, 94.6206; H, 5.4299.

2.2. Electrochemical characterization

The electrochemical properties of PPCA and BDA were characterized by means of cyclic voltammetry. The oxidation scans were carried out in a 0.1 M solution of tetraethylammonium tetrafluoroborate in anhydrous CH_2Cl_2. A platinum and Ag/AgCl disk were used as the working and reference electrodes, respectively. Specifically, the platinum disk was used as the counter electrode. Based on the highest occupied molecular orbital (HOMO) energy of the ferrocene/ferrocenium redox system (-4.8 eV), we were able to calculate the HOMO energy values of PPCA and BDA which were both equal to 5.6 eV. The band-gap energies were measured from the absorption spectra, and the lowest unoccupied molecular orbital (LUMO) energies were estimated to be equal to 2.6 eV for PPCA and 2.8 eV for BDA. The energy levels of PPCA and BDA indicate that Förster resonance energy transfer (FRET) takes place between the host (PPCA) and the dopant (BDA), because as shown in Fig. 4 the band-gap energy of PPCA is greater than that of BDA (see Supporting Information) [21,22].

2.3. OLED fabrication

OLEDs were fabricated by means of vacuum deposition onto patterned ITO glasses that had been thoroughly cleaned and subsequently, treated with oxygen plasma. Blue OLEDs were sequentially fabricated onto the ITO substrates through thermal evaporation of organic layers (evaporation rate: 2 Å/s; base pressure: 3×10^{-6} Torr). The EL spectra and CIE color coordinates were obtained using a Spectrascan PR650 photometer, while the current–voltage–luminescence (J–V–L) characteristics were measured using a Keithley 2400 source unit.

3. Results and discussion

3.1. Synthesis

Scheme 1 shows the synthetic route to PPCA. Specifically, the Pd-catalyzed Suzuki coupling reaction of 9-bromoanthracene with 9-phenanthreneboronic acid afforded **1** in 87% yield. Bromination of **1** with 1.01 equiv. of bromine in chloroform solution led to the formation of **2** in 89% yield. **2A** was synthesized through the reaction of 3-bromo-9-phenylcarbazole with 1.1 equiv. of n-BuLi at −78 °C and subsequent quenching of the lithiated complex with triethylborate. PPCA was synthesized through a Pd-catalyzed Suzuki coupling reaction, similarly to the case of **1**.

Scheme 2 shows the synthetic route to BDA. Specifically, **4** was synthesized according to a previously described procedure [16]. A suspension of 2,6-dibromoanthraquinone in Et_2O was slowly added to lithium-substituted biphenyl in order to obtain **3**. The latter was aromatized using NaH_2PO_2 and KI to obtain **4** in 84% yield. The next step was to obtain BDA through the Pd-catalyzed Suzuki-coupling reaction of **4** with phenylboronic acid in 2 M aqueous K_2CO_3 solution. The molecular structures of PPCA and BDA were characterized by means of ^{1}H NMR, mass spectrometry, and elemental analysis (EA).

3.2. Thermal properties and quantum yields

The thermal behavior of BDA and PPCA was evaluated by means of (a) differential scanning calorimetry (DSC) and (b) thermogravimetric analysis (TGA) under a nitrogen atmosphere. A 5% weight loss was observed at 398 and 367 °C. The melting point (T_m) of BDA and PPCA was 396 and 326 °C and the decomposition temperature (T_d) was 445 and 440 °C, respectively. These data indicate that both these materials are stable enough to endure the high temperature at which the vacuum vapor deposition is carried out (see Supporting Information).

Additionally, the fluorescence quantum yield (Φ) was measured using the standard optically diluted method in CH_2Cl_2 solution and 9,10-diphenylanthracene (Φ = 0.90, in CH_2Cl_2) as the reference standard. The fluorescence quantum yield of BDA and PPCA were 0.74 and 0.83, respectively [23,24].

3.3. Optical properties of PPCA and BDA

Fig. 1 shows the UV absorption and PL spectra of PPCA and BDA dissolved in dichloromethane as well as in the

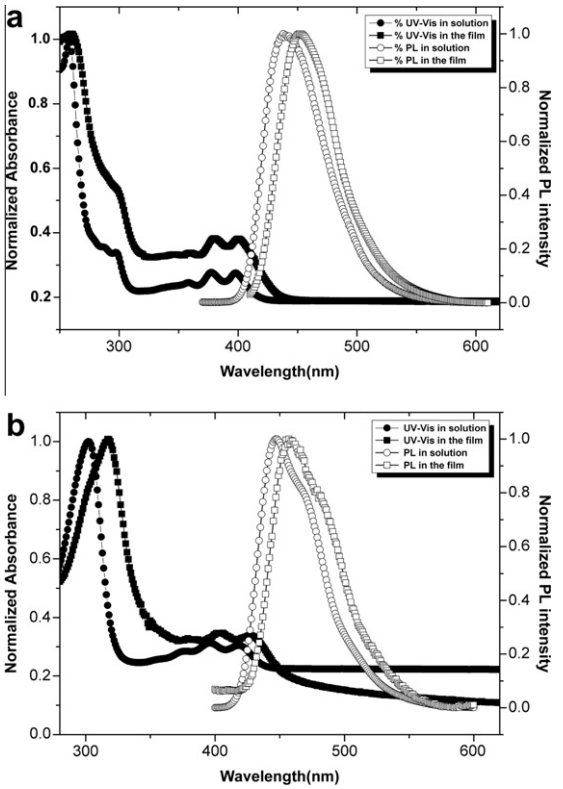

Fig. 1. UV absorption and PL spectra of PPCA and BDA dissolved in dichloromethane (CH_2Cl_2) and in the case of solid thin films deposited on a quartz substrate. (a) Normalized UV absorption and PL spectrum of PPCA. (b) Normalized absorption and PL spectrum of BDA.

form of solid thin films. Specifically, two major bands are observed in the UV absorption spectra of the material dissolved in dichloromethane and in the form of solid thin films (Fig. 1a). The first strong absorption, which is observed at a wavelength of 258 nm with a shoulder peak at 300 nm, can be attributed to the 9-phenyl-9H-carbazole moiety. The absorption peaks observed at a wavelength of 358 nm, 378 nm, and 398 nm are associated with the vibronic features of the anthracenyl core [25]. Upon photoexcitation, the PL emission of PPCA dissolved in the dichloromethane peaked at a wavelength of approximately 438 nm and at 452 nm in the case of the solid thin film. The spectral shift in solid state is due to the different dielectric constant of the surrounding medium [26].

In Fig. 1b, the absorption peaks of BDA dissolved in dichloromethane show vibrational patterns at a wavelength of 373 nm, 396 nm, and 419 nm, which are typical to aryl-substituted anthracene [16,20]. The maximum PL of BDA dissolved in dichloromethane was observed at a wavelength of 448 nm and at 456 nm in the case of the solid thin film. Additionally, in the host-dopant system, the probability of energy transfer from the excited energy donor to the energy acceptor depends on the overlap of the emission spectrum of the donor with the absorption spectrum of the acceptor. This is evident from the spectral overlap between the PL of PPCA and the UV absorption of BDA (see Supporting Information) [27–32].

3.4. EL properties and OLED characteristics

Fig. 2 shows the structures of Alq_3 and N1PP acting as electron-transporting materials and the EL spectra of the 5% doped devices driven at 10 mA/cm^2. To elucidate the energy transfer from PPCA to BDA, we fabricated two kinds of multilayer structures: ITO/DNTPD (600 Å)/α-NPB (300 Å)/

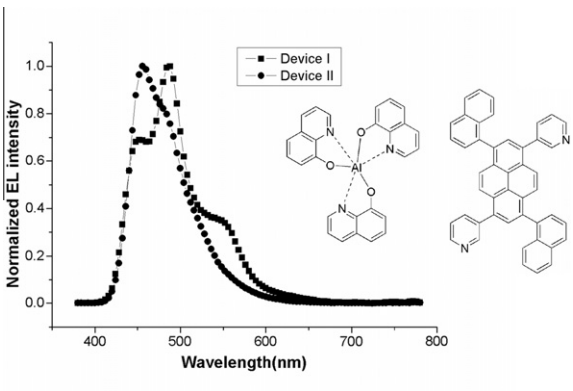

Fig. 2. EL spectra of Device I and II along with the structures of Alq_3 and N1PP.

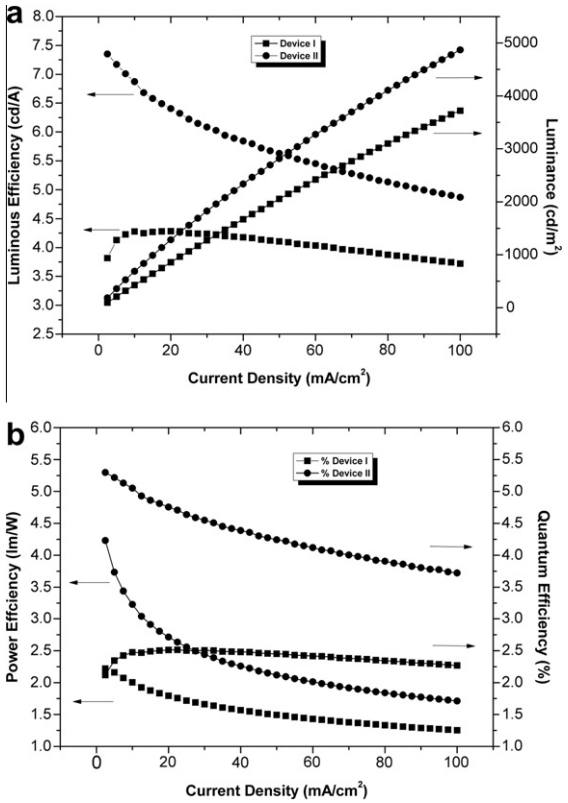

Fig. 3. EL performance of Device I and II. (a) The current–efficiency and density–luminance characteristics of Device I and II. (b) The power efficiency–current density–external quantum efficiency characteristics of Device I and II.

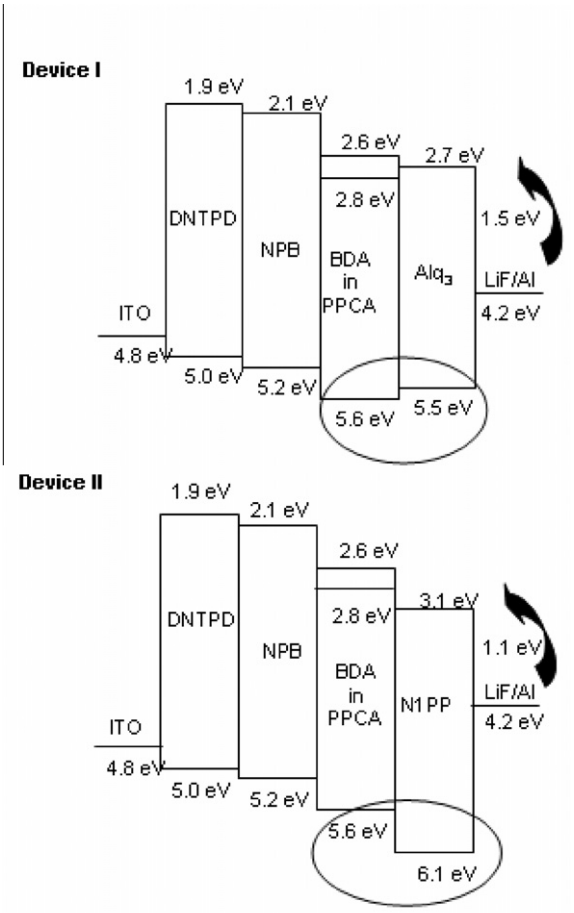

Fig. 4. HOMO and LUMO energy levels of the materials used for the fabrication of Device I and II.

PPCA:BDA 5 wt.% (250 Å)/Alq_3 (300 Å)/LiF (5 Å)/Al (1000 Å) (Device I) and ITO/DNTPD (600 Å)/α-NPB (300 Å)/PPCA:BDA 5 wt.% (250 Å)/N1PP (300 Å)/LiF (5 Å)/Al (1000 Å) (Device II). We used *N,N′*-di(4-*N,N′*-diphenylamino)phenyl)-*N,N′*-diphenylbenzidine (DNTPD) as the hole-injection layer (HIL), 4,4′-bis[*N*-(1-napthyl)-*N*-phenylamino]biphenyl (α-NPB) as the hole-transport layer (HTL), PPCA as the fluorescent blue host, BDA as the fluorescent blue dopant, N1PP and Alq_3 as the electron-transport layers (ETL) [19], and LiF as the electron-injection layer (EIL) at the LiF/Al cathode interface. The EL spectrum of Device I, in which Alq_3 was used as an ETL, was found to be different from that of Device II, which used N1PP as an ETL. In Device I, three major peaks were observed at a wavelength of 454 nm, 487 nm, and 525 nm. We believe that the two higher energy emissions are due to BDA, while the lower energy emission is due to Alq_3 [33–35].

The experimental results suggest that energy transfer takes place between the light-emitting and the electron-transporting layer. Specifically, a peak in the blue-light emission of Device II was observed at a wavelength of 456 nm, which is almost identical to that of the PL spectrum of BDA in the form of a solid thin film (Fig. 1b). This coincidence indicates that while the light emission of PPCA (host) is essentially quenched in the light emitting layer of the 5% doped device, FRET takes place between the host (PPCA) and the dopant (BDA) [35,36].

Fig. 3 shows the EL performance of Devices I and II, while their EL efficiencies are summarized in Table 1. Specifically, Device I showed a current efficiency of 4.30 cd/A, power efficiency of 2.00 lm/W, and an external quantum efficiency of 2.50% at 10 mA/cm^2 (at CIE coordinates of (0.15, 0.28)). Device II, on the other hand, delivered a better performance with a current efficiency of 6.90 cd/A, power efficiency of 3.23 lm/W, and external quantum efficiency of 5.10% at 10 mA/cm^2 (at CIE coordinates of (0.15, 0.18)).

To further verify the difference between the EL performances of Device I and II, we examined their band-gap energies. Fig. 4 show the HOMO and LUMO energy levels of the organic material, along with the work functions of their metal layers. This energy diagram reveals that the energy barrier (1.5 eV) between the EIL (4.2 eV) and ETL (Alq_3) (2.7 eV) in Device I is larger than the difference (1.1 eV) between the electrode and N1PP (3.1 eV) in Device II [19] Since Alq_3 is characterized by a higher LUMO level than N1PP, electron injection from the LiF/Al cathode into the 5% doped emission layer is rather difficult to be achieved in Device I. Furthermore, the difference between the HOMO values of the emitting layer (EML) and the ETL will cause leakage of holes from the 5% doped emitting zone into the ETL (Alq_3). In Device I, the HOMO level (5.5 eV) of Alq_3 is higher than that of PPCA (5.6 eV). This difference can explain why the electron–hole recombination may be unbalanced in the emitting zone of Device I. This unbalanced charge recombination also shifts the blue light-emitting zone to a region close to the ETL (Alq3) (Fig. 4) and therefore, Device I delivers a poor performance. On the other hand, the HOMO level of N1PP (6.1 eV) is lower than that of PPCA (5.6 eV). Because of the energy barrier (0.5 eV) between the HOMO level of PPCA (5.6 eV) and that of N1PP (6.1 eV), N1PP can act as a hole blocker preventing holes from leaking into the ETL. This behavior suggests that since N1PP has better carrier-transporting and hole-blocking characteristics, it facilitates electron–hole recombination in the 5% doped emitting zone. Consequently, the EL performance of Device II is superior to that of Device I.

Table 1
Summary of the characteristics of Devices I and II with Alq_3 and N1PP as an ETL.

Device	EL peak [nm]	Current efficiency @10 mA/cm^2 [cd/A]	Luminance @10 mA/cm^2 [cd/m^2]	Power efficiency @10 mA/cm^2 [lm/W]	External quantum efficiency [%]	CIE coordinates [*x,y*]
Device I	487	4.30	428/3720[a]	2.00	2.50	0.15, 0.28
Device II	456	6.90	687/4869[a]	3.23	5.10	0.15, 0.18

[a] Measured at 100 mA/cm^2.

4. Conclusions

In summary, we have synthesized new anthracene-based host (PPCA) and dopant (BDA) materials and used them to fabricate efficient blue OLEDs. PPCA carries an electron-transporting 9-phenanthrene moiety as well as a hole-transporting 9-phenyl-9H-carbazole moiety in the anthracene core. On the other hand, BDA consists of PAHs without amino substituents in the anthracene core. Charge balance could be achieved by using N1PP as the electron-transporting material. The device with the optimized structure, ITO/DNTPD (600 Å)/α-NPB (300 Å)/PPCA:BDA 5 wt.% (250 Å)/N1PP (300 Å)/LiF (5 Å)/Al (1000 Å) (Device II), is characterized by high blue EL performance with a current efficiency of 6.9 cd/A, a power efficiency of 3.23 lm/W, and an external quantum efficiency of 5.1% at 10 mA/cm^2 at CIE coordinates of (0.15, 0.18). This study shows that π-conjugated anthracene-functionalized PAHs without amino substituents can be used as efficient dopants for blue OLEDs.

Acknowledgments

This study was supported by the Basic Science Research Program through a National Research Foundation of Korea (NRF) grant funded by the Ministry of Education, Science and Technology (MEST) of Korea for the Center for Next-Generation Dye-sensitized Solar Cells (No. 2010-0001842).

Appendix A. Supplementary data

Supplementary data associated with this article can be found, in the online version, at doi:10.1016/j.orgel.2011.02.011.

References

[1] J. Shi, C.W. Tang, Appl. Phys. Lett. 80 (2002) 3201.
[2] P.-I. Shih, C.-Y. Chuang, C.-H. Chien, Diau, W-G. Eric, C-F. Shu, Adv. Funct. Mater. 17 (2007) 3141.
[3] C.-H. Chien, C.-K. Chen, F.-M. Hsu, C.-F. Shu, P.-T. Chou, C.-H. Lai, Adv. Funct. Mater. 19 (2009) 560.
[4] J.-H. Jou, Y.-P. Lin, M.-F. Hsu, M.-H. Wu, P. Lu, Appl. Phys. Lett. 92 (2008) 193313.
[5] K.-R. Wee, H.-C. Ahn, H.-J. Son, W.-S. Han, J.-E. Kim, D.-W. Cho, S.-O. Kang, J. Org. Chem. 74 (2009) 8472.
[6] B.M. Krasovitskii, B.M. Bolotin, Organic Luminescent Materials translated by V.G. Vopian, VCH, Weinheim, 1988.
[7] V.V. Jarikov, J. Appl. Phys. 100 (2006) 014901.
[8] R.J. Tseng, R.C. Chiechi, F. Wudl, Y. Yang, Appl. Phys. Lett. 88 (2006) 093512.
[9] B.K. Shah, D.C. Neckers, J. Shi, E.W. Forsythe, D. Morton, Chem. Mater. 18 (2006) 603.
[10] V.V. Jarikov, D.Y. Kondakov, C.T. Brown, J. Appl. Phys. 102 (2007) 104908.
[11] M.-T. Lee, C.-H. Liao, C.-H. Tsai, C.-H. Chen, Adv. Mater. 17 (2005) 2493.
[12] K. Danel, T.-H. Huang, J.-T Lin, Y.-T. Tao, C.-H. Chuen, Chem. Mater. 14 (2002) 3860.
[13] M.–H. Ho, Y.-S. Wu, S.-W. Wen, T.-M. Chen, C.-H. Chen, Appl. Phys. Lett. 91 (2007) 083515.
[14] P.-I. Shih, C.-Y. Chuang, C.-H. Chien, E.W.G. Diau, C.-F. Shu, Adv. Funct. Mater. 17 (2007) 3141.
[15] M.X. Yu, J.P. Duan, C.H. Lin, C.H. cheng, Y.T. Tao, Chem. Mater. 14 (2002) 3958.
[16] W.-J. Jo, K.-H. Kim, H.-C. No, D.-Y. Sim, S.-J. Oh, J.-H. Son, Y.-H. Kim, S.-K. Kwon, Synth. Met. 159 (2009) 1359.
[17] H.-Y. Chen, C.-Ti. Chen, C-Tsen. Chen, Macromolecules 43 (2010) 3613.
[18] H.W. Hung, N. Yokoyama, M. Yahiro, C. Adachi, Thin Solid Films 516 (2008) 8717.
[19] H.Y. Oh, C. Lee, S. Lee, Org. Electron. 10 (2009) 163.
[20] Li Li, J.-H. Zou, J. Huang, C. Li, Y. Zhang, C. Sun, X-H. Zhu, J. Peng, Y. Cao, J. Ronchali, Org. Electron. 9 (2008) 649.
[21] J. Wang, Y.D. Jiang, J.S. Yu, Appl. Phys. Lett. 91 (2007) 131105.
[22] K. Okumoto, Y. Shirota, Chem. Mater. 15 (2003) 699.
[23] S. Tao, S. Xu, X. Zhang, Chem. Phys. Lett. 429 (2006) 622.
[24] Z. Yang, Z. Chi, L. Zhou, X. Zhang, M. Chen, B. Xu, C. Wang, Y. Zhang, J. Xu, Opt. Mater. 32 (2009) 398.
[25] J.B. Lagowski, THEOCHEM 589–590 (2002) 125–137.
[26] J. Salbeck, F. Weissörtel, N. Yu, J. Bauer, H. Bestgen, Synth. Met. 91 (1997) 209.
[27] C. Adachi, M.A. Baldo, M.E. Thopmson, S.R. Forrest, J. Appl. Phys. 90 (2001) 5048.
[28] M.-S. Kim, B.-K. Choi, T.-W. Lee, D.S. Shin, S.K. Kang, J.M. Kim, S. Tamura, Appl. Phys. Lett. 91 (2007) 251111.
[29] Y. Zhang, G. Cheng, S. Chen, Y. Li, Y. Zhao, S. Liu, F. He, L. Tian, Y. Ma, Appl. Phys. Lett. 88 (2006) 223508.
[30] F. Li, M. Zhang, G. Cheng, J. Feng, Y. Zhao, Y. Ma, S. Liu, J. Shen, Appl. Phys. Lett. 84 (2004) 148.
[31] K.H. Lee, Y.S. Kwon, L.K. Kang, G.Y. Kim, J.H. Seo, Y.K. Kim, S.S. Yoon, Synth. Met. 159 (2009) 2603.
[32] J.K. Park, K.H. Lee, S. Kang, J.Y. Lee, J.S. Park, J.H. Seo, Y.K. Kim, S.S. Yoon, Org. Electron. 11 (2010) 905.
[33] E.-M. Han, L.-M. Do, N. Yamamoto, M. Fujihira, Thin Solid Films 273 (1996) 202.
[34] M.A. Baldo, D.F. O'Brien, M.E. Thompson, S.R. Forrest, Phys. Rev. B 60 (1999) 14422.
[35] M.-T. Lee, H.-H. Chen, C.-H. Liao, C.-H. Tsai, C.H. Chen, Appl. Phys. Lett. 85 (2004) 3301.
[36] S.O. Jeon, K.S. Yook, C.W. Joo, J.Y. Lee, Adv. Funct. Mater. 19 (2009) 3644.